

## Electrochemical assessment of calcium carbonate deposition using a rotating disc electrode (RDE)

A. NEVILLE<sup>1</sup>, T. HODGKIESS<sup>2</sup> and A. P. MORIZOT<sup>1</sup>

<sup>1</sup>*Department of Mechanical and Chemical Engineering, Heriot-Watt University, Edinburgh, EH14 4AS Scotland;*

<sup>2</sup>*Department of Mechanical Engineering, Glasgow University, Glasgow, Scotland*

Received 20 March 1998; accepted in revised form 28 September 1998

*Key words:* carbonate, cathodic, deposition, electrochemical, inhibitors, rotating disc electrode, scaling

### Abstract

An electrochemically-based technique, which uses assessment of the oxygen reduction reaction at a rotating disc electrode, has been devised which shows promise as a method for studying nucleation and growth of mineral scale at a solid surface. In this paper the background and development of the technique are described for the study of deposition of CaCO<sub>3</sub> from a supersaturated solution. Results are presented which illustrate the good correlation between the surface coverage predicted by electrochemical analysis and the actual coverage quantified by image analysis. The potential of this technique for mechanistic studies of surface scaling and for assessment of inhibitors is discussed.

### 1. Introduction

Deposition of mineral scales (e.g., CaCO<sub>3</sub>, CaSO<sub>4</sub>, BaSO<sub>4</sub>) is a serious practical problem in many process industries [1–4]. Deposition of CaCO<sub>3</sub>, poses particular problems on heated surfaces in, for example, cooling water systems and desalination plants [5, 6].

A vast amount of research has been conducted into three principal areas: kinetics of precipitation, prediction models and inhibitor development and technology [e.g., 7–10]. As a result, there have been significant advances in the understanding of precipitation and in the control of scaling. However, scaling continues to impose massive costs to process industries, particularly in the oil industry where access to fouled components for acid cleaning or replacement requires costly shut-down.

Studies of scale kinetics to date have primarily focused on assessment of the kinetics of homogenous and heterogeneous precipitation in the bulk solution. Indeed existing scaling indices (e.g., Langelier, Stiff–Davis and Odde–Tomson saturation indices) are based on extensive experimentation of bulk scaling parameters [11, 12]. Numerous corrections for temperature, pressure and ionic concentration have been devised to be applied to the above indices [13]. In recent work by

Hasson et al. [14] it was stated that more effort should be directed to scaling kinetics at solid surfaces since it has been demonstrated [15] that there are often wide anomalies between actual deposition and rates estimated by predictive models based on scaling indices.

In this paper the development of a novel technique based on an electrochemically active rotating disc electrode (RDE) for the study of kinetics and inhibition of scaling on a solid surface is described. Results are presented which demonstrate that accurate measurement of the extent of surface scale can be achieved by electrochemical assessment of the oxygen reduction reaction (Equation 1). In addition, information regarding the nature of the scale formed, in terms of its ability to block the surface, can be obtained by correlation of electrochemical parameters and surface examination.



### 2. Theory and background

The study is based on the correlation between the diffusional characteristics of oxygen at a surface and the changes in the rate of oxygen reduction once nucleation

and growth of  $\text{CaCO}_3$  occurs. The technique is based on the analysis of mass transport to the surface of a rotating disc electrode (RDE). The development of mass transport equations was first performed by Levich [16]. Adams covers the theories developed by Levich in relation to a wide range of electrode processes [17]. The benefit of the RDE over other flow and diffusion control methods is the ability to obtain precisely controlled hydrodynamic conditions which are uniform over the entire electrode surface. In the present work, the RDE was used to obtain controlled conditions of convective diffusion to the electrode surface. Mass transfer analysis can be integrated into a hydrodynamic analysis to develop a relation between the limiting current for a reaction under mass transport control and the rotational speed via Equation 2.

$$i_L = 0.62 n F A C^b D^{2/3} \nu^{-1/6} \omega^{1/2} \quad (2)$$

where  $i_L$  is the limiting current (mA),  $\omega$  the angular velocity of the RDE ( $\text{rad s}^{-1}$ ),  $C^b$  the bulk concentration of electroactive species ( $\text{mol dm}^{-3}$ ),  $\nu$  the kinematic viscosity ( $\text{cm}^2 \text{s}^{-1}$ ),  $F$  the Faraday's constant ( $96487 \text{ C equiv}^{-1}$ ),  $A$  the electrode area ( $\text{cm}^2$ ),  $n$  the number of electrons involved in electrode reaction, and  $D$  the diffusion coefficient of the electroactive species ( $\text{cm}^2 \text{s}^{-1}$ ).

The rate of the oxygen-reduction cathodic reaction (Equation 1) is limited by mass transport of dissolved oxygen molecules to the electrode surface. This is manifested during potentiodynamic cathodic polarization tests as a diffusion plateau where the electrochemical current reaches a limiting steady state value  $i_L$ , virtually independent of overpotential.

The linear relationship between the limiting current ( $i_L$ ) and  $\omega^{1/2}$  has been widely used in the determination of diffusion coefficients in mass transport controlled systems. The above analysis is valid for reactions under mass transport control. However, several studies have been carried out in systems where there is mixed mass transport and charge transfer control. In such circumstances the  $i_L$  against  $\omega^{1/2}$  relationship is no longer a straight line and, as the rotation speed increases, the divergence from linearity increases. This is due to the fact that at low rotational velocities, diffusion effects are controlling whereas, as the rotational speed increases, the rate of electrochemical transformation can have an overall effect on the reaction kinetics.

The technique described here relies on the distinction between the *active* surface area on a bare and scaled electrode. Figure 1 is a simple representation of discrete crystals on a surface where  $A_o$  is the total active surface

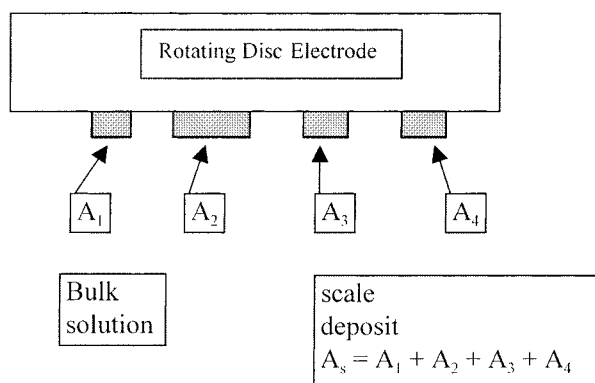


Fig. 1. Schematic of electrode indicating active sites in the presence of scale deposition.

area of the bare electrode and  $A_s = A_1 + A_2 + A_3 + A_4$  is the reduced active surface area once scale crystals have deposited.

The following assumptions are made in the development of the technique:

- (i) electrochemical reactions occur only on the exposed surface, free from scale (i.e. the scale does not allow oxygen transport through the crystal lattice)
- (ii) the corrosion reaction of the substrate with the electrolyte has a negligible effect on the results of the experiment
- (iii) deposits do not redissolve at any point during the analysis once precipitated
- (iv) oxygen reduction takes place at a constant rate over the surface and the diffusion coefficient of oxygen to the active sites is constant for bare and scaled electrodes.

The development of the technique presented here was driven by the need to focus research towards the operational problem involved in mineral scale formation, namely deposition on a functional surface. The approach adopted enhances the scope for understanding of fundamental aspects of scale formation and the mechanisms by which inhibitors act on or interact with the metal surface to slow down nucleation or growth of scale crystals. It is regarded as complementary to the wealth of information gained from bulk chemistry measurements.

### 3. Experimental details

The experimentation used in the development and validation of the technique involved three phases. First, the chemistry of the scaling solution had to be decided, secondly the electrochemical control method and oxy-

gen reduction reaction kinetics had to be characterized and, finally, the electrochemistry had to be integrated into the surface scaling study.

Calcium carbonate scales were nucleated and grown on the surface of a stainless steel (UNS S31603) electrode in a solution of  $\text{Na}_2\text{CO}_3$  and  $\text{CaCl}_2$ . Equal amounts of  $\text{Na}_2\text{CO}_3$  and  $\text{CaCl}_2$  were added to make a supersaturated solution; this solution is referred to as the scaling solution. The solution was maintained at a temperature of  $25^\circ\text{C}$  and pH of 10.0 by addition of NaOH to negate the pH decrease due to the solubility of  $\text{CO}_2$  from the surrounding atmosphere and precipitation of  $\text{CaCO}_3$ . The index of supersaturation,  $I_s$ , was 235, estimated using activity coefficients calculated using the extended Debye–Huckel expressions [18]. The formation of  $\text{CaCO}_3$  in the bulk solution was followed by recording the amount of NaOH added as a function of time. Figure 2 shows a typical plot in which the NaOH required to maintain a pH of 10.0 increases during precipitation until a steady value is reached. This corresponds to the completion of bulk precipitation. These results will not be considered to any great extent in this paper but comparison of bulk/surface scaling kinetics and inhibition is the focus of another communication [19]. The trend of the plot of volume of NaOH added against time was validated using measurement of turbidity and  $\text{Ca}^{2+}$  ion concentration. As can be seen from Figure 2, the increase in turbidity and in  $\text{Ca}^{2+}$  ion concentration correspond very well with the trend of increasing volume of NaOH required during precipitation. The bulk precipitation kinetics were therefore followed in the remainder of the work by recording the

volume of NaOH added to maintain the pH at the fixed level.

The formation of  $\text{CaCO}_3$  scale at the electrode surface was achieved by immersion of the sample in the supersaturated solution for a fixed period. Once the scale had been generated, the analysis relied on assessing the electrochemical parameters of the surface compared with the scale-free surface using a standard RDE set-up comprising a potentiostatically controlled three-electrode electrochemical cell in which the rotating disc specimen forms the working electrode. In order that the surface could be analysed without further precipitation or dissolution during the analysis period, the electrochemical assessment was carried out in a saturated solution ( $I_s = 1$ ) comprising  $\text{Na}_2\text{CO}_3$  and  $\text{CaCl}_2$ . This solution also contained NaCl to increase the conductivity required for electrochemical measurements. The conductivity of this solution was  $9\text{ mS cm}^{-1}$  and the pH was maintained at 10. This solution is referred to hitherto as the analysis solution.

The electrodes comprised 9.9 mm diameter bar of stainless steel UNS S31603 grade which was then inserted into a 11 mm diameter polymer sleeve. This eliminated hydrodynamic edge effects at the RDE surface and achieved uniform accessibility of the reactants.

Preliminary tests on precipitate-free samples were carried out in the analysis solution to determine the oxygen reduction reaction kinetics of the stainless steel electrode as a function of applied cathodic potential. It is well established that the controlling factor in the reduction of oxygen in aerated solutions is concentration polarization, indicated by a diffusion plateau on a cathodic polarization curve. In this concentration limited region, the oxygen reduction current is limited by the rate of supply of oxygen to the surface and is therefore under diffusion control. Potentiodynamic cathodic polarization tests were carried out at 0 rpm and rotation speeds of 400, 800 and 1200 rpm. The potential was scanned at a rate of  $15\text{ mV min}^{-1}$  using a computer controlled potentiostat. A platinum electrode served as auxiliary electrode and the reference electrode used for all the tests was a saturated calomel electrode (SCE). Figure 3 shows the clear diffusion plateaux at the different rotational speeds. From this information it was decided that the potential of  $-1\text{ V vs SCE}$  would be used as the potentiostatic control potential for surface scale analysis.

The electrode potential for potentiostatic analysis ( $-1\text{ V vs SCE}$ ) is more electronegative than the equilibrium potential for hydrogen ion reduction and in principle this reaction could occur. However, in preliminary tests to choose the appropriate potential for

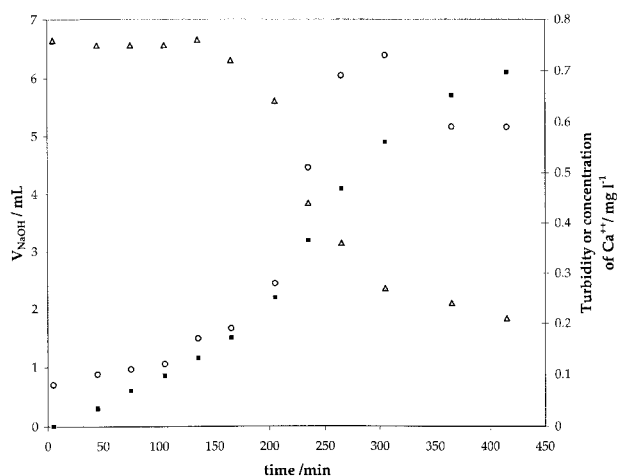


Fig. 2. Relationship between turbidity, amount of NaOH added to maintain the pH at 10 and the  $\text{Ca}^{2+}$  concentration in the bulk solution. Key: (■) volume of NaOH added; (▲) concentration of  $\text{Ca}^{2+}$  in the bulk; (○) turbidity.

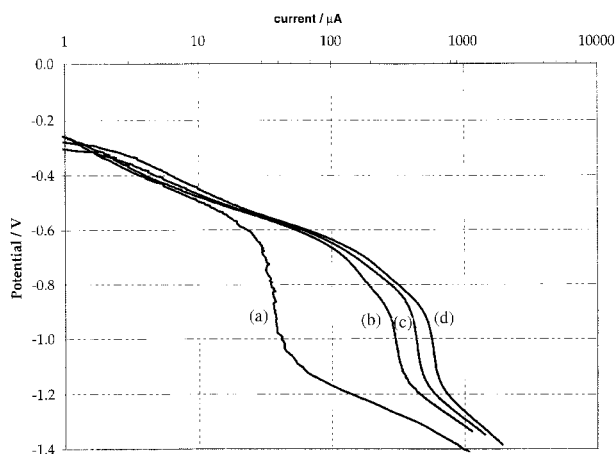


Fig. 3. Cathodic polarization in the analysis solution at different velocities. Key: (a) static; (b) 400 rpm; (c) 800 rpm; (d) 1200 rpm.

electrochemical analysis, potentiodynamic sweeps were performed in deaerated water to ascertain the effect of the hydrogen ion reduction reaction on the measured current at a potential of  $-1$  V. This was found to be 0.5% of the total current at 1200 rpm and was therefore considered to be of little significance for the analysis.

Integration of the electrochemical characterisation of the surface to determine the extent of scaling was then possible by the following experimental procedure. The unscaled electrode was polarized cathodically into the diffusion plateau region, at a potential of  $-1$  V vs SCE and the current was measured as a function of the rotational speed. The rotating disc electrode speed was measured via a tachometer and the current versus speed results were recorded over a range of speeds typically between 600 rpm and 2500 rpm over which the accuracy of the speed control was optimum ( $\pm 2$  rpm). The samples were then placed in the scaling solution which was continuously stirred using a magnetic stirrer. Once the scale had been deposited over a predetermined period, the samples were again immersed in the saturated analysis solution and the sample was polarized to  $-1$  V vs SCE and the corresponding data for limiting current ( $i_L$ ) against rotational speed ( $\omega$ ) were obtained.

Analysis of the electrochemical data in the form of a graph of  $i_L$  against  $\omega^{1/2}$  on the electrode, before and after scale deposition, yields the apparent percentage change in active area once scale has formed. Scanning electron microscopy, with integrated image analysis, was then used to analyse the morphology of the crystals formed and, in particular, verify the actual percentage surface coverage of the electrode. X-ray diffraction (XRD) was used to determine the crystallographic form of the deposit.

The time for scale to nucleate and grow on the surface in the scaling solution was between 5 min and 3 h. Variations in the sample position in the scale solution altered the extent of scaling at the surface and coverages in the range 5–60% were achieved. Further immersion of the sample in a low supersaturated solution ( $I_s = 40$ ) enhanced the deposition and coverages in excess of 90% were achieved. Measurement of the amount of  $\text{CaCO}_3$  deposited was undertaken by a spectrophotometric hardness method to give concentration of  $\text{Ca}^{2+}$  ions in mg/l present as  $\text{CaCO}_3$ .

## 4. Results

### 4.1. Extent of scaling

It became apparent very early in the study that surface preparation of the electrodes was critical to ensure the achievement of consistent  $i_L$  against  $\omega^{1/2}$  relationships before any scale was deposited. Changes in the surface roughness achieved by abrasion using 800 grit SiC paper compared with 1200 grit paper were very significant. Electrodes were first abraded using 800 and 1200 grit SiC paper and then polished to a  $6 \mu\text{m}$  finish using a diamond compound.

The consistency of the results for the initial Levich plot was then good as shown in Figure 4 for three unscaled electrodes. The deviation in the gradient was not more than 1% for the three electrodes and this was

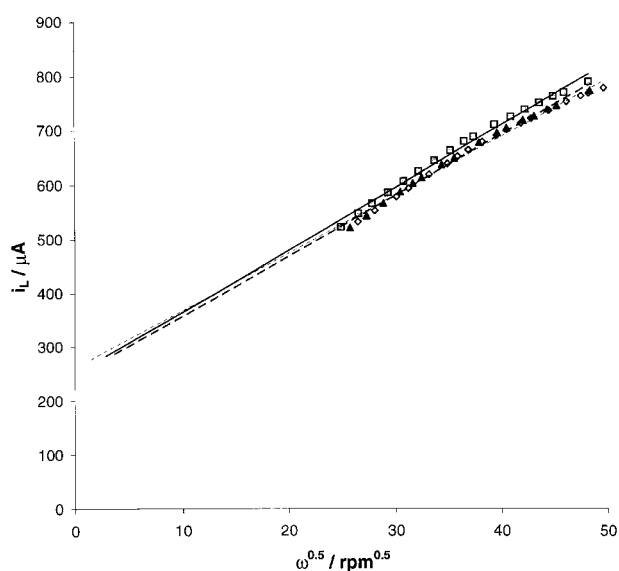


Fig. 4. Levich analysis (plot of  $i_L$  against  $\omega^{0.5}$ ) on bare electrodes showing good reproducibility and linear fit. Key: ( $\diamond$ ) 1st electrode; ( $\blacktriangle$ ) 2nd electrode; ( $\square$ ) 3rd electrode; (----) linear, 1st electrode; (---) linear, 2nd electrode; (—) linear, 3rd electrode.

reproduced in each of the subsequent experiments. As can be seen in Figure 4, the  $i_L$  against  $\omega^{1/2}$  plot is a good linear fit indicating that the reduction of oxygen at the electrode is under sole mass transport control in accordance with Equation 2. With the entire surface uniformly accessible on the bare electrode, the Levich relationship was used to calculate the value for the diffusion coefficient for oxygen. This was found to be ( $1.1 \times 10^{-5} \text{ cm}^2 \text{ s}^{-1}$ ) which is in agreement with typical values in the literature [20].

Deposition under the conditions in this study consistently yielded the vaterite polymorph of  $\text{CaCO}_3$  which comprised ellipsoidal crystals. Vaterite is a metastable form of  $\text{CaCO}_3$  usually formed as a precursor to calcite [21]. As such there have been fewer reported studies of its formation. However, as stated by Kralj et al. [22], it is of importance in the study of nonequilibrium precipitation processes. For this study the form of  $\text{CaCO}_3$  was not of great importance since the main purpose was to validate the electrochemical method for determining the extent of scale deposition on the metal surface.

Figure 5(a), (b) and (c) show the Levich response for three electrodes onto which scale had deposited by prior immersion in the scaling solution. Analysis of the gradient of the  $i_L$  against  $\omega^{1/2}$  line enabled the surface coverage as a percentage of the original surface area to be calculated by

$$\text{coverage} = \frac{m_1 - m_2}{m_1} \times 100$$

where  $m_1$  and  $m_2$  are the gradients of the  $i_L$  against  $\omega^{1/2}$  plot for the unscaled (initial) and scaled (final) electrodes, respectively. The three electrodes in Figure 5(a), (b) and (c) were thus found to have 8%, 33% and 51% surface coverage, respectively.

The deposited scale was confirmed by microscopy to be essentially a layer of one-crystal thickness and this did not alter the controlling parameter for the oxygen-reduction reaction as indicated in Figure 5(a), (b) and (c). The  $i_L$  against  $\omega^{1/2}$  relationship was still linear, although the correlation coefficient was lower than on the unscaled specimen. Thus the reaction was still primarily controlled by mass transfer effects.

Image analysis of the scaled surfaces was performed on 16 samples, the extent of scaling being different on each sample due to variations in immersion time and position in the scaling solution. Calculation of the coverage of scale was done by an image analysis package in which the proportion of projected area covered by vaterite crystals was calculated as a percentage of the entire surface area. Figure 6 shows the relationship between surface coverage determined by electrochemical assessment of the oxygen-reduction reaction kinetics

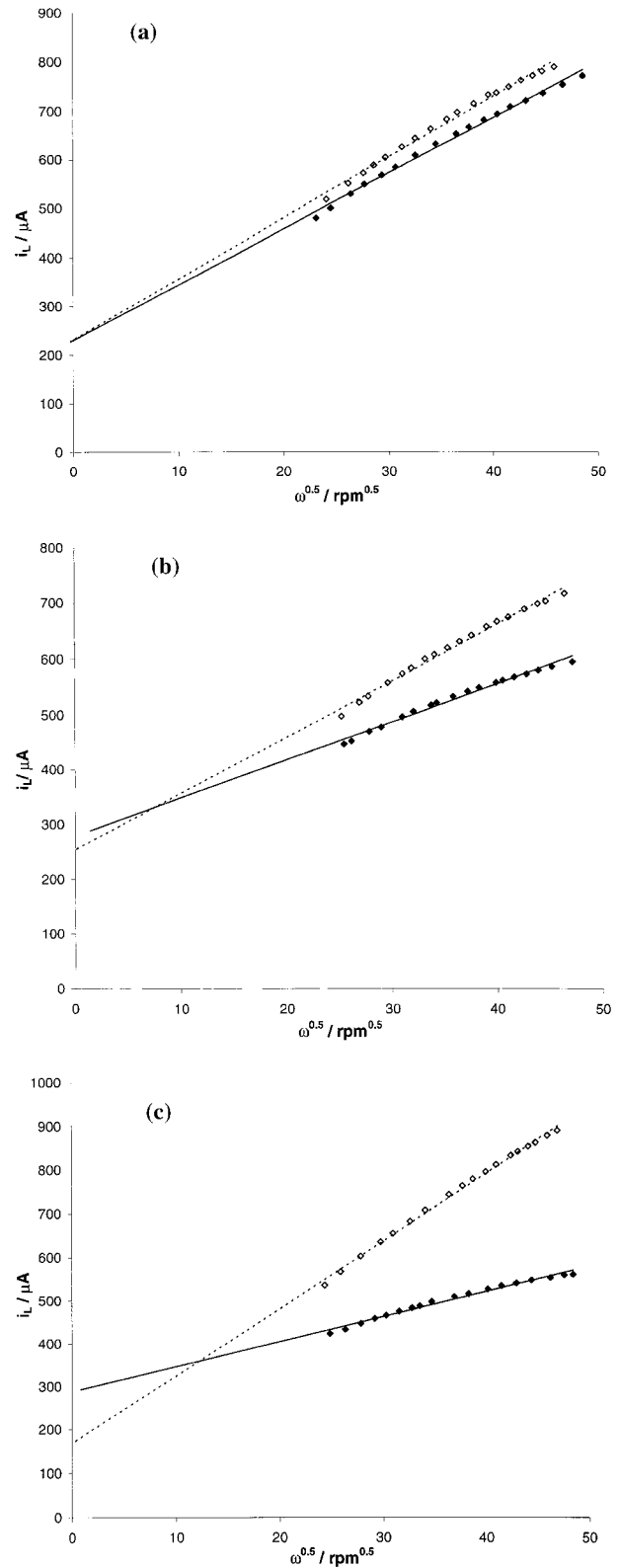


Fig. 5. Levich plots for bare and scaled specimens (a) 8% scaling coverage, (b) 33% and (c) 51% coverage. Key: ( $\diamond$ ) initial; ( $\blacklozenge$ ) final; (----) linear, initial; (—) linear, final.

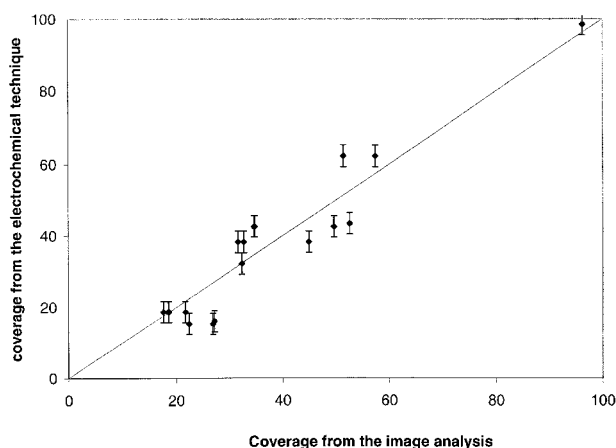


Fig. 6. Correlation of coverage by electrochemical means and image analysis. Key: (◆) experimental data; (—)  $y = x$ .

and the coverage as detected by the image analysis over the range of coverage spanning 5–90%. As can be seen there is generally a good correlation with some deviation at lower levels of scaling.

#### 4.2. Scaling regimes

Figure 7 shows the relationship between the surface coverage of scale (determined by Levich analysis) and the amount of scale deposited in  $\text{mg dm}^{-3}$  (determined

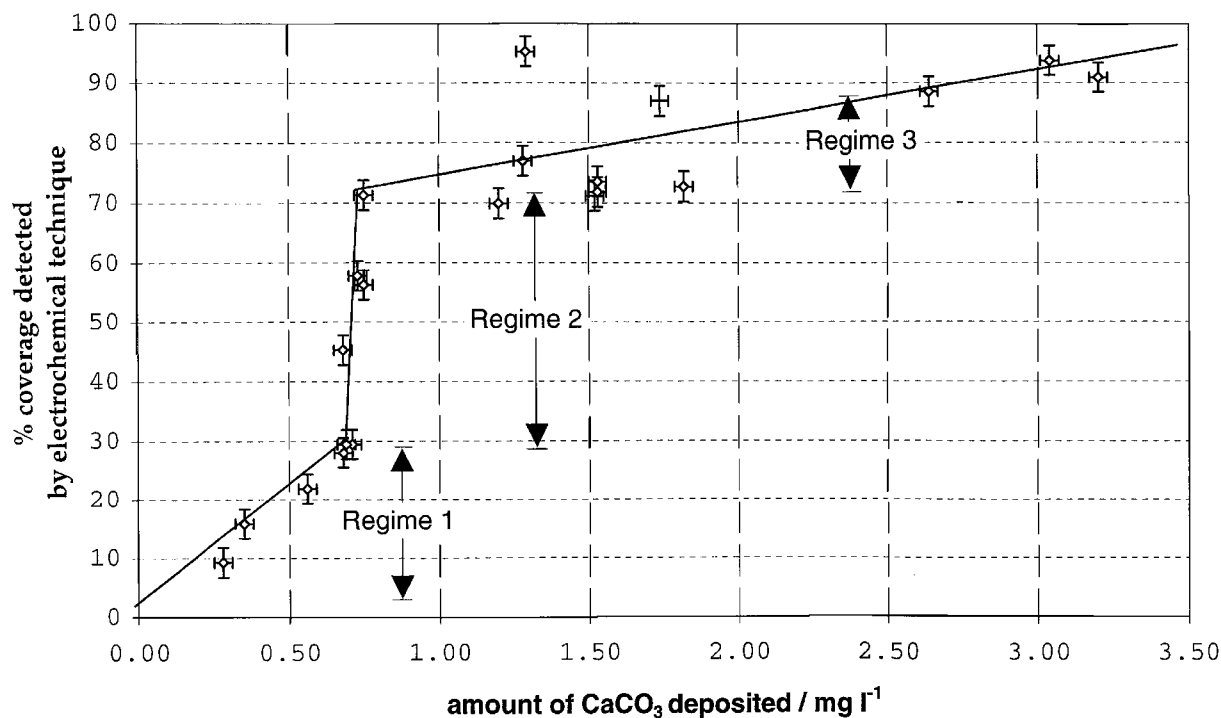


Fig. 7. Different regimes detected by correlation of amount of precipitate on the surface and the surface coverage detected electrochemically.

Table 1. Crystal characteristics in the three regimes identified by electrochemical analysis

Regime	Scale characteristics
1	Larger crystals. Intercrystal spacing larger. Figure 8.
2	More smaller crystals than above. Figure 9.
3	Range of crystal sizes from small nuclei to large crystals. Some overlapping. Figure 10.

by dissolution of the scale followed by a  $\text{Ca}^{2+}$  analysis) for a number of electrodes. There are three distinct regimes and microscopic examination enabled the three regimes to be correlated to the nature of the scale deposited. Regimes 1 and 2 resulted from immersion in only the first scaling solution whereas scale generated in regime 3 was as a result of immersion in the second solution of lower supersaturation. The characteristics of the scale are summarized in Table 1.

It was noted that there appeared to be less nucleation sites in regime 1 than in regime 2 but that growth was stimulated in regime 1. As such the layer in regime 1 was more porous since the gaps between the crystals was greater. The trends shown in Figure 7 have no time dependence but what is important is the ability of the electrochemical assessment to be used in conjunction with quantification of the mass of deposit to provide information on the extent of nucleation and/or growth at a surface.

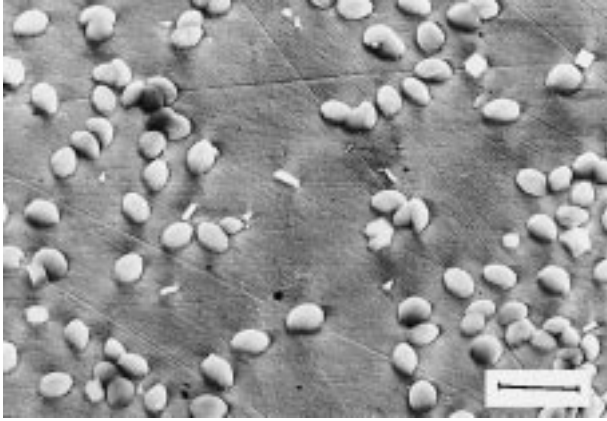


Fig. 8. Scale characteristics in regime 1. Large crystals with large intercrystal spacing. Scale bar = 10  $\mu\text{m}$ .

## 5. Discussion

Studies of the kinetics of mineral scale formation have primarily focused on determining processes involved in the bulk solution rather than on solid surfaces. Much information therefore exists on nucleation and growth mechanisms and kinetics in the bulk solution but significantly less information exists relating to scale formation on a solid surface. Validation of inhibitors for use in scale control systems for plant relies primarily on information generated from bulk scaling studies. Hasson et al. [14] recently stated that in practice the formation of scale on industrial plant surfaces often does not follow the kinetics predicted by beaker tests on bulk solution chemistry. Recently there has been an increased effort to address this by the authors and others [19, 23]. A.c. impedance has been used as a tool for

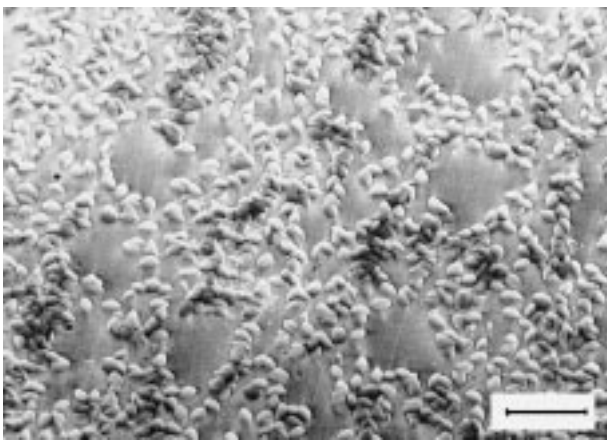


Fig. 9. Scale characteristics in regime 2. More, smaller crystals than in Figure 8. Scale bar = 10  $\mu\text{m}$ .

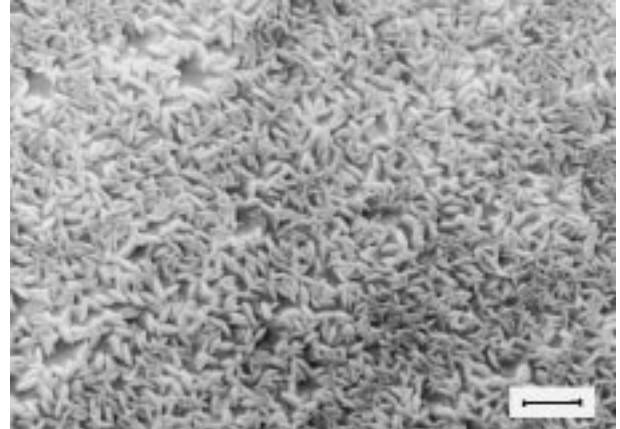


Fig. 10. Scale characteristics in regime 3. Some overlapping crystals. Scale bar = 10  $\mu\text{m}$ .

predicting and assessing scale layers formed on steel surfaces with some degree of success [23].

The current study has demonstrated that, by following the kinetics of the oxygen reduction reaction at a rotating disc electrode surface, the extent of surface coverage of mineral  $\text{CaCO}_3$  deposits can be accurately determined. The correlation between the surface coverage determined by electrochemical means and that determined by image analysis is good, the results being more accurate as the surface coverage increases. Two possible causes of the slightly poorer correlation at low surface coverages are now discussed. The first involves a consideration of the geometrical form of the crystals in this study. Ellipsoidal vaterite was formed as previously shown. In the assessment of the surface coverage by image analysis the projected area was calculated but as shown in the schematic representation in Figure 11, the three dimensionality of the scaling means that the actual surface coverage in terms of the inactive area could be a lot less than predicted by the projected area. The regions under the ellipsoid will not wholly be in contact with the surface and as such there is scope for oxygen reduction underneath the crystals, albeit at a lower rate than on the free surface. This is not accounted for in the

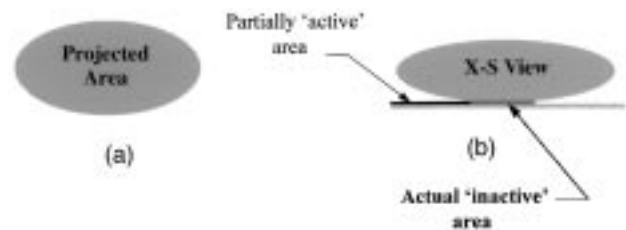


Fig. 11. Schematic of the contact area of vaterite on the surface which is less than the projected area detected by image analysis. Key: (a) area detected by image analysis; (b) actual situation.

assumptions made to develop the model. Hence the prediction of the amount of coverage by image analysis is more than the actual inactive area by consideration of electrochemical oxygen reduction. This is more evident at lower scaling levels since as crystals coalesce the regions beneath become less electrochemically active. The second point to consider in the analysis is that the technique used for determination of the surface coverage electrochemically relies on the entire surface being uniformly accessible for oxygen reduction. The presence of crystals will induce local turbulence effects, a point noted by Levich in his original analysis. This can have two effects: first, the microscopically rough surface will affect the local nature of the velocity boundary layer thus changing the hydrodynamics and, secondly, the turbulence associated with individual crystals will enhance the supply of oxygen to the regions near to the crystals. These features will result in a slight under estimation of surface coverage by the Levich analysis shown in Figure 6.

As mentioned previously the  $i_L$  against  $\omega^{1/2}$  relationship, once scaling has occurred exhibits a small degree of nonlinearity not evident on the bare electrode as is clear in Figure 5(a), (b) and (c). However the general trend is still linear and a good correlation coefficient of greater than 0.99 is obtained. This indicates that the overall controlling mechanism is mass transport as on the bare electrode but would suggest that the introduction of a nonuniform layer onto the surface is inducing some instabilities. For the layers studied in this work, this has not affected the correlation between surface coverage deduced by electrochemical and image analysis methods. However, as more extensive scale layers are obtained the Levich analysis may well deviate further from a linear response.

The ability to accurately determine the extent of scale deposition on a metal surface by electrochemical means is an important development in the fundamental and practical aspects of scaling. A particularly promising avenue of study using the electrochemical technique pertains to the assessment of scale inhibitors. Some preliminary work in this area [19, 24] has indeed indicated the potential of the method for measuring, directly on a surface, the influence of inhibitors on retarding scale deposition. Moreover, it appears that the results of Levich analyses, together with the other measurements described herein (microscopy and bulk-solution analysis), can yield important clues as to the mechanisms of surface inhibition. A comparison of the effect of an inhibitor on bulk and surface kinetics can also be made. The electrochemical technique also opens up several other possible directions into which the work could be extended such

as detailed study is the effect of hydrodynamics ion scale deposition in uninhibited and inhibited environments.

## 6. Conclusions

A novel electrochemical technique to address the fundamental aspects of scaling at a solid surface has been introduced. It has been demonstrated to accurately predict the extent of surface deposition and to enable the characteristics of the scale to be determined. As a tool for integrating the study of bulk chemistry and surface scaling kinetics in uninhibited and inhibited environments in a variety of industrial applications, the technique shows great potential.

## References

1. J.N. Kennedy, NL Industries, (1972).
2. C.K. Walker, L.C. Fraser and B.L. Dibrell, Corrosion '94, paper 52, Houston, TX (NACE, 1994).
3. C.M. Shaughnessy and W.E. Kline, *J. Petroleum Technol.* (Oct., 1973) 1783–91.
4. C. Patton, 'Water Applied Technology', edited by J.M. Campbell, 1st edn. Campbell Petroleum Series (1986).
5. S.D. Strauss, *Power*. (Sept. 1992) 17–20.
6. A.H. Tuthill, *Power Eng.* (July) 39–42.
7. R.G. Compton and P.J. Daly, *J. Colloid Interface Sci.* **115** (Febr. 1987) 493–8.
8. L.N. Morgenthaler, Z.I. Khatib, R.N. French and K.R. Cox, *Mater. Perform.* (Apr. 1991) 37–42.
9. G.E. Geiger, *Hydrocarbon Process.* (Jan. 1996) 93–8.
10. S. Patel and A.J. Nicol, *Mater. Perform.* (June 1996) 41–6.
11. W.F. Langelier, *J. Amer. Water Works Assoc.* **38** (1936) 1500.
12. H.A. Stiff and L.E. Davies, *Trans. AIME* **195** (1952) 213.
13. J.E. Oddo and M.B. Thomson, *J. Petrol. Technol.* (July 1982) 1583.
14. D. Hasson, D. Bramson, B. Limoni-Relis and R. Semiat, *Desalination*, **108** (1996) 67–79.
15. A. Harris and A. Marshall, Proceedings of the symposium on 'Progress in the Prevention of Fouling', Nottingham, 1981, p. 174.
16. B.G. Levich, *Acta Physicochimica URSS* **17** (1942) 257.
17. R.N. Adams, 'Electrochemistry at Solid Electrodes', (Dekker, 1969).
18. L.N. Plummer and E. Busenberg, *Geochim. Cosmochim. Acta* **46** (1982) 1011–40.
19. A.P. Morizot, A. Neville and T. Hodgkiess, submitted to *J. Crystal Growth*.
20. R.E. Davies, G.L. Horvath and C.W. Tobias, *Electrochim. Acta* **12** (1966) 287–97.
21. D. Chakraborty, V.K. Agarwal, S.K. Bhatia and J. Bellare, *Ind. Eng. Chem. Res.* **33** (1994) 2187–97.
22. D. Kralj and L. Brecevic, *J. Crystal Growth* **104** (1990) 793–800.
23. C. Gabrielli, M. Keddam, G. Maurin, H. Perron, R. Rosset and M. Zidoune, *J. Electroanal. Chem.* **412** (1996) 189–93.
24. A. Neville, T. Hodgkiess and A.P. Morizot, Corrosion '98, paper 65, San Diego, TX, NACE (1998).